A Compact Physics Analytical Model for Hot-Carrier Degradation

Stanislav Tyaginov, Alexander Grill, Michiel Vandemaele, Tibor Grasser, Geert Hellings, Alexander Makarov, Markus Jech, Dimitri Linten, and Ben Kaczer

***Abstract*—We develop and validate a fully analytical model for hot-carrier degradation based on a thorough description of the physical picture behind this reliability phenomenon. This approach captures and links carrier transport, modeling of the Si-H bond-breakage mechanisms, and simulations of the degraded devices. All quantities evaluated within the model are described by analytical expressions and time consuming TCAD simulations are therefore avoided. We show that the model can capture measured dependencies of the normalized linear drain current change on stress time with good accuracy.**

***Index Terms*—Hot-carrier degradation, analytical model, compact model, interface traps, carrier transport**

I. Introduction

Among the reliability issues plaguing modern FETs, hot-carrier degradation (HCD) is being continuously reported to be the most detrimental one [1, 2] and therefore device time-to-failure during HC stress should be accurately modeled and predicted. Simplified techniques, which rely on backward extrapolation of time-to-failure from aggressive stress conditions to milder operating regimes using a simple analytical expression, fail to capture the entire complexity of HCD [3]. Although physics-based models for HCD [4–11] have reached a high level of maturity, they are typically computationally very challenging and therefore not suitable for circuit and system level reliability simulations. Within these models, the most computationally expensive part is carrier transport, required for obtaining the carrier energy distribution functions (DFs) and then the Si-H bond dissociation rates.

To tackle this problem, we recently proposed a methodology for modeling the carrier DFs using an analytical formula with parameters obtained from drift-diffusion simulations [12–14]. This strategy allows one to avoid the time consuming solution of the Boltzmann transport equation (BTE), obtain the carrier DFs, which accurately represent populations of hot and cold carriers, and reproduce degradation traces. However, this model still relies on the drift-diffusion approach to the BTE solution and requires a TCAD device simulator. In addition to this, simulations of the degraded devices also require a drift-diffusion solver. Another approach, which links a compact model of current-voltage characteristics with a description of carrier and defect generation rates, was presented in our recent publication [15]. However, the main deficiency of this approach is that calculations of Si-H bond-breakage rates are based on the electric field profile which is obtained from drift-diffusion simulations. To summarize, this makes these aforementioned models not perfectly suitable for reliability modeling at the circuit level.

To bridge this gap, we develop and validate an analytical model for HCD which does not rely on the drift-diffusion approach but still can represent HCD degradation traces with good accuracy; this model is implemented into the gate stack analyzer Comphy, which is a compact physics simulator of reliability issues in semiconductor devices [16].

S. Tyaginov is with with *imec*, Leuven 3001, Belgium, also with the Institute for Microelectronics, Technische Universität Wien, 1040 Vienna, Austria, and also with the Ioffe Physical-Technical Institute, Russian Academy of Sciences, 194021 Saint-Petersburg, Russia.

A. Grill and M. Vandemaele are with KU Leuven, Department of Electrical Engineering (ESAT), MICAS, Kasteelpark Arenberg 10, 3000 Leuven, Belgium and also with *imec*, Leuven 3001, Belgium.

G. Hellings, D. Linten, and B. Kaczer are with *imec*, Leuven 3001, Belgium.

A. Makarov, M. Jech, and T. Grasser are with the Institute for Microelectronics, Technische Universität Wien, 1040 Vienna, Austria.

II. Devices and Experiment

To validate the proposed model we used n-channel planar MOSFETs with a gate length of 65 nm and an operating voltage of $V_{\rm dd}$ = 1.2 V. As the gate dielectric, an SiON layer with a physical thickness of 2.5 nm, formed using a decoupled plasma nitridation followed by a postnitridation anneal, was employed. These devices were stressed at $V_{\rm gs}$ = $V_{\rm ds}$ = 1.8 and 2.0 V ($V_{\rm gs}$ and $V_{\rm ds}$ are gate and drain voltages, correspondingly) for $\sim$9 ks at room temperature. Note that the combination $V_{\rm gs}$ = $V_{\rm ds}$ corresponds to the worst-case condition of HCD in short-channel transistors. During stress, the normalized changes of the linear drain current $\Delta I_{\rm d,lin}$ ($I_{\rm d,lin}$ corresponds to the current at $V_{\rm ds}$ = 0.05 V and $V_{\rm gs}$ = 1.2 V) as functions of stress time t were recorded.

III. The Model Structure

Our modeling framework captures and links three main aspects of HCD: carrier transport, calculation of the defect generation rates, and modeling of the degraded devices (see Fig. 1). In the TCAD implementation of our HCD model, carrier transport is covered by the deterministic Boltzmann transport equation solver ViennaSHE [17], employed to calculate the carrier energy DFs. As for the defect generation process, we consider two mechanisms of Si-H bond rupture, namely single- and multiple-carrier (SC- and MC-) mechanisms; their rates are evaluated using information of the carrier DFs. Finally, to simulate the characteristics of the degraded devices we employ the device simulator MINIMOS-NT [18] within the GTS framework [19], which uses drift-diffusion and hydrodynamic approaches to the Boltzmann transport equation solution combined with quantum corrections.

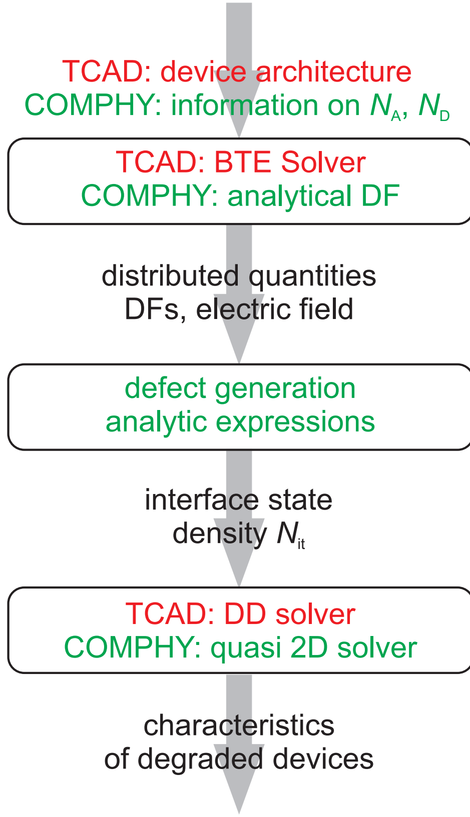

Fig. 1. Schematic representation of our HCD modeling framework. Flowcharts for TCAD and Comphy versions of the model are marked with red and green colors, respectively.

In the proposed version of the HCD model we aim at substituting all TCAD simulations – which require a significant computational resources – by more efficient compact physics based solutions. This strategy is sketched in Fig. 1, where the ingredients related to the compact physics model and the TCAD approach are highlighted by green and red colors, respectively. As its essential part, the module of degraded device modeling includes also simulation of pristine devices; this task is tackled by representing the device as a sequence of several slices and assuming that within each slice all electrostatic and transport quantities keep constant (see Fig. 2). The information about carrier concentration and carrier temperature in undamaged FETs is needed to evaluate the carrier DFs.

IV. Carrier Transport

Carrier energy distribution functions $f(\varepsilon)$ (ε is the carrier energy) are described using the *analytical expression* proposed in [20], which models the populations of both hot and cold carriers:

$$f(\varepsilon) = A\exp\left[-\left(\frac{\varepsilon}{\varepsilon_{\mathrm{ref}}}\right)^{b}\right] + C\exp\left[-\frac{\varepsilon}{k_{\mathrm{B}}T_{L}}\right], \quad (1)$$

where the exponent b is assigned a value of 2, k_{B} is the Boltzmann constant, T_{L} the lattice temperature, and T_{n} denotes the carrier temperature obtained using the electric field in Si (F_{Si}) and the carrier mobility μ as

$$T_n = T_{\mathrm{L}} + \frac{2}{3}\frac{q}{k_{\mathrm{B}}}\tau_{\mathrm{E}}\mu F_{\mathrm{Si}}^2 \quad (2)$$

with the quantity τ_{E} being the energy relaxation time. The parameters A, C and $\varepsilon_{\mathrm{ref}}$ in (1) are found using the normalization criteria to represent the carrier concentration n, carrier temperature T_n, and the kurtosis β_{k} (also found from device modeling):

$$\int_0^\infty f(\varepsilon)g(\varepsilon)d\varepsilon = n \quad (3)$$

$$\int_0^\infty \varepsilon f(\varepsilon)g(\varepsilon)d\varepsilon = \frac{3}{2}nk_{\mathrm{B}}T_{\mathrm{n}} \quad (4)$$

$$\frac{3}{5}\frac{\langle\varepsilon^2\rangle}{\langle\varepsilon\rangle^2} = \frac{3}{5}\frac{n\int_0^\infty \varepsilon^2 f(\varepsilon)g(\varepsilon)d\varepsilon}{\left(\int_0^\infty \varepsilon f(\varepsilon)g(\varepsilon)d\varepsilon\right)^2} = \beta_{\mathrm{k}} \quad (5)$$

Note that for the density-of-states an analytical formula which mimics the Kane dispersion relation (as suggested in [20]) is used

$$g(\varepsilon) = g_0\sqrt{\varepsilon}\,(1+\eta\varepsilon) \quad (6)$$

with η = 1.404 eV^{-1} being the nonparabolicity factor and the parameter g_0 is determined as

$$g_0 = \frac{6m^*\sqrt{2m^*}}{\pi^2\hbar^3} \quad (7)$$

with m^* being the electron effective mass and $\hbar$ the normalized Planck's constant.

The kurtosis β_{k} is given by empirical formulas derived from Monte Carlo simulation results by Grasser *et al.* [20]:

$$\beta_{\mathrm{k}}(T_{\mathrm{n}}) = \frac{T_{\mathrm{L}}^2}{T_{\mathrm{n}}^2} + 2\frac{\tau_\beta}{\tau_\varepsilon}\frac{\mu_{\mathrm{S}}}{\mu}\left(1-\frac{T_{\mathrm{L}}}{T_{\mathrm{n}}}\right), \quad (8)$$

where τ_ε, τ_β, μ, and μ_{S} are the energy relaxation time, the kurtosis relaxation time, the electron mobility, and the energy flux mobility. Calculation of parameters τ_ε, τ_β, and μ_{S} is a

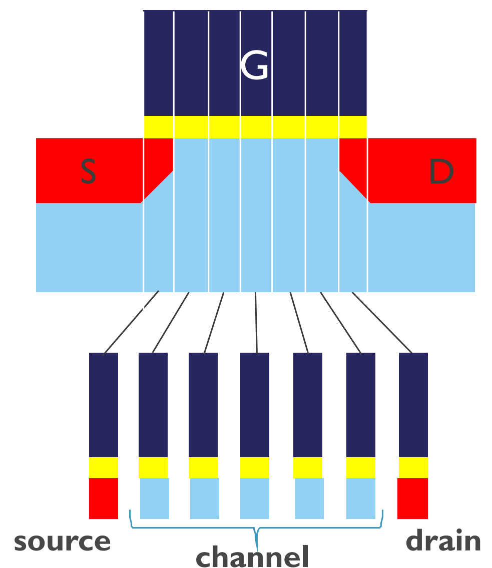

Fig. 2. Schematic representation of a FET divided into slices.

very non-trivial task but fortunately the prefactor on the right hand side in (8) can be described by an empirical analytical expression proposed in [20]:

$$2\,\frac{\tau_\beta}{\tau_\varepsilon}\,\frac{\mu_\mathrm{S}}{\mu} = x_0 + x_1\left[1-\exp\left(-x_2\,\frac{T_\mathrm{L}}{T_\mathrm{n}}\right)\right] \tag{9}$$

with $x_0 = 0.69$, $x_1 = 1.34$, $x_2 = 1.89$ being dimensionless parameters.

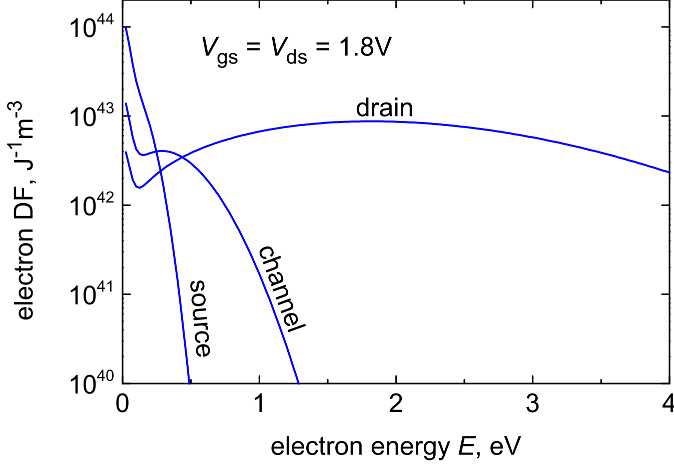

Fig. 3. Electron energy DFs calculated with the analytical expression (1) for $V_\mathrm{gs} = V_\mathrm{ds} = 1.8$ V.

Electron DFs calculated with this formalism are shown in Fig. 3. One can see that at the source cold carriers follow a Maxwellian distribution, while in the channel and at the drain the DFs are severely non-equilibrium, consistent with our previous results [12, 13].

It is noteworthy that the carrier DFs are described by simple analytical expressions, which in turn lead to analytical formulas for the bond-breakage rates (see Section V). Moreover, these DFs can be used to model non-equilibrium bias temperature instability (BTI), that is, BTI at $V_\mathrm{ds} \neq 0$ when charging of oxide traps is driven by hot carriers [21].

It is important to emphasize that the only fragment in the carrier DF calculation requiring a numerical solution is the system (3)-(5) which determines the parameters A, C and ε_ref. However, this is a simple system of algebraic equations, the solution of which is not time consuming.

V. Defect Generation

The calculation of interface state generation rates is performed by considering all superpositions of single- and multiple-carrier mechanisms of Si-H bond rupture [9, 10]. The rates of both mechanisms are described by the carrier acceleration integral

$$I_\mathrm{SC|MC} = \int_{E_\mathrm{th}}^{\infty} f(\varepsilon)g(\varepsilon)\sigma_\mathrm{SC|MC}(\varepsilon)v(\varepsilon)d\varepsilon \tag{10}$$

with the Keldysh-like reaction cross section for the rates of both SC- and MC-mechanisms

$$\sigma_\mathrm{SC|MC}(\varepsilon) = \sigma_\mathrm{0,SC|MC}\,\left[(\varepsilon-\varepsilon_\mathrm{th})/1\,\mathrm{eV}\right]^{p_\mathrm{SC|MC}}, \tag{11}$$

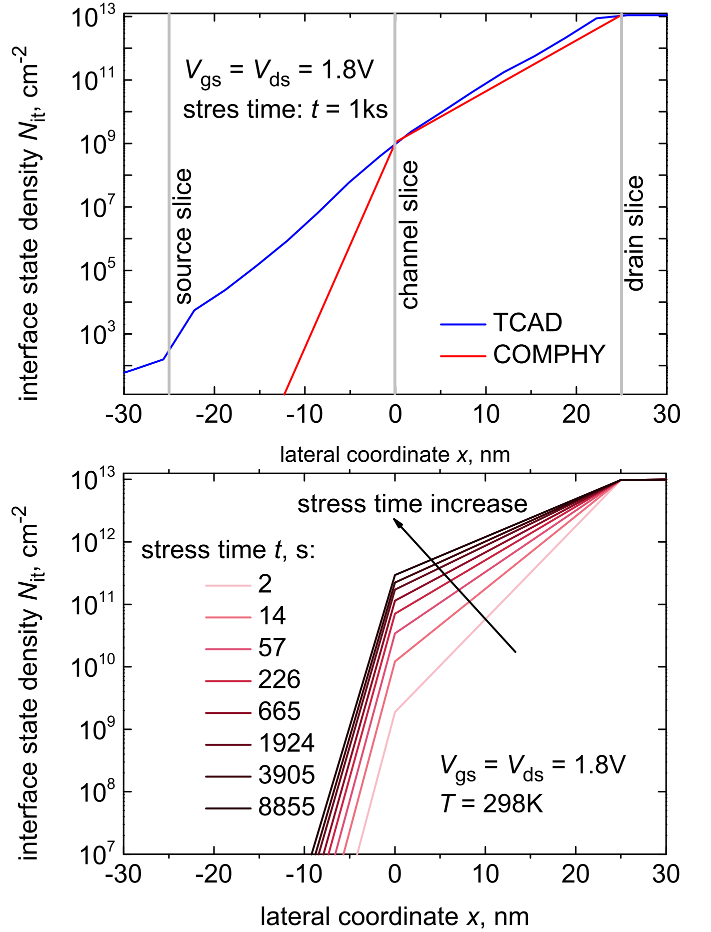

Fig. 4. Upper panel: comparison of $N_\mathrm{it}(x)$ profiles obtained with the BTE solution (TCAD) and the analytical model (Comphy); lower panel: evolution of $N_\mathrm{it}(x)$ profiles with stress time t evaluated using Comphy.

where the exponents p_SC and p_MC are equal to 11 and 1, correspondingly [22, 23]. The energy ε_th is equal to the bond-breakage energy $E_\mathrm{a} = 2.56\,\mathrm{eV}$ [24] in case of the SC-mechanism and the distnace between the eigenstates the Si-H bond $\hbar\omega = 0.25\,\mathrm{eV}$ for the MC-mechanism [10]. As for the prefactors $\sigma_\mathrm{0,SC|MC}$, their values are summarized in Fig. 5.

With the carrier DFs expressed by (1), the DOS given by (6), and reaction cross sections determined by (11), the acceleration integral (10) can thus be expressed by combinations of Γ-functions, i.e. by analytical formulas. Then, the interface state density N_it is also given by an analytical expression:

$$\begin{aligned} N_\mathrm{it}(t) &= \frac{\sqrt{R_\mathrm{a}^2/4+N_0R_\mathrm{a}\widetilde{R}_\mathrm{p}}}{\widetilde{R}_\mathrm{p}}\,\frac{1-\widetilde{f}(t)}{1+\widetilde{f}(t)} - \frac{R_\mathrm{a}}{2\widetilde{R}_\mathrm{p}},\\ \widetilde{f}(t) &= \frac{\sqrt{R_\mathrm{a}^2/4+N_0R_\mathrm{a}\widetilde{R}_\mathrm{p}}-R_\mathrm{a}/2}{\sqrt{R_\mathrm{a}^2/4+N_0R_\mathrm{a}\widetilde{R}_\mathrm{p}}+R_\mathrm{a}/2}\times\\ &\qquad\times\exp\left(-2t\sqrt{R_\mathrm{a}^2/4+N_0R_\mathrm{a}\widetilde{R}_\mathrm{p}}\right) \end{aligned} \tag{12}$$

with the generalized bond dissociation and passivation rates

Parameter	TCAD Model	Compact Physics Model
SC process cross section, $\sigma_{0,\mathrm{SC}}$	$5\times10^{-18}\,\mathrm{cm}^2$	$1.5\times10^{-17}\,\mathrm{cm}^2$
MC process cross section, $\sigma_{0,\mathrm{MC}}$	$5\times10^{-19}\,\mathrm{cm}^2$	$7\times10^{-19}\,\mathrm{cm}^2$
Mean value of the bond-breakage energy, $\langle E_\mathrm{a}\rangle$	2.56 eV	2.56 eV
Standard deviation of the bond-breakage energy, σ_E	0.35 eV	0.37 eV
Density of pristine Si-H bonds, N_0	$1.2\times10^{13}\,\mathrm{cm}^{-2}$	$1.2\times10^{13}\,\mathrm{cm}^{-2}$

Fig. 5. The model parameters used in TCAD and compact physics versions of the HCD model. One can see that capture cross sections of SC and MC processes used in these two versions are slightly different but all other parameters are the same.

R_a, R_p:

$$\begin{aligned} R_\mathrm{a} &= \frac{1}{k_\mathrm{norm}}\sum_i R_{\mathrm{a},i}\left(\frac{P_\mathrm{u}}{P_\mathrm{d}}\right)^i, \\ R_\mathrm{p} &= \nu_\mathrm{p}\exp\left(-\frac{E_\mathrm{pass}}{k_\mathrm{B}T_\mathrm{L}}\right). \end{aligned} \tag{13}$$

Let us briefly discuss that the Si-H bond is modeled within the truncated harmonic oscillator model and the index i in the expression for the bond rupture rate R_a enumerates the bonded levels; the parameter k_norm is needed for the normalization criterion of the level population numbers which are determined by bond excitation/deexcitation rates P_u, P_d. The energy for the backward, passivation, reaction E_pass is equal to 1.5 eV and agrees well with the values reported in experimental papers [25–27]). The rates P_u, P_d they are given by these expressions:

$$\begin{aligned} P_\mathrm{u} &= \omega_\mathrm{e}\exp\left(-\hbar\omega/k_\mathrm{B}T_\mathrm{L}\right) + I_\mathrm{MC}, \\ P_\mathrm{d} &= \omega_\mathrm{e} + I_\mathrm{MC}, \end{aligned} \tag{14}$$

where $\hbar\omega$ is the distance between the oscillator levels and $1/\omega_\mathrm{e}$ = 1.5 ns is the lifetime of the stretching vibrational mode of the bond (we consider bond dissociation via the MC mechanism to occur via the stretching mode [10]). For more details, please refer to [22, 23].

The components $R_{\mathrm{a},i}$ entering (13) are the contributions to the cumulative bond dissociation rate from bonded levels enumerated by the index i:

$$R_{\mathrm{SP},i} = w_\mathrm{th}\exp\left[-\left(E_\mathrm{a}-E_i\right)/k_\mathrm{B}T_\mathrm{L}\right] + I_{\mathrm{SC},i}, \tag{15}$$

where the first term represents the Arrhenius rate for the thermal activation of the potential barrier between the level i with the corresponding energy E_i and the transport mode (with the attempt frequency w_th), while the second term corresponds to the bond dissociation triggered by a solitary hot carrier:

$$I_{\mathrm{SC},i}(E_\mathrm{a}) = \int f(\varepsilon)g(\varepsilon)\sigma_0(\varepsilon - E_\mathrm{a} + E_i)^{p_\mathrm{it,SP}}v(\varepsilon)\mathrm{d}\varepsilon. \tag{16}$$

Fig. 4, upper panel shows good agreement between $N_\mathrm{it}(x)$ profiles (x is the coordinate along the Si/dielectric interface) calculated using the current model and full TCAD treatment with DFs obtained as a solution of the BTE, while the lower panel depicts the evolution of the concentration N_it with time. Note that in the drain region HCD is quite strong, i.e. all available Si-H bonds are dissociated and N_it is saturated (a detailed discussion is given in [28]).

Let us finally emphasize that *all expressions needed to calculate the density* N_it *(10)-(14) are fully analytic*.

VI. Modeling of pristine devices

For simplified device modeling, we divide the transistor into slices, as sketched in Fig. 2. It is noteworthy that we already employed this slicing in [15] but the electric field profile was still evaluated using the drift-diffusion approach to the Boltzmann transport equation solution. Within each slice, the electric field, doping concentration, carrier density, mobility, and temperature, etc. are assumed to be constant. For each slice i we convert the doping concentration into a resistivity and then evaluate the potential drop $\Delta V_{\mathrm{ds},i}$ in the lateral direction caused by the applied V_ds. After that, the gate voltage V_gs applied to this slice is corrected by the value $\Delta V_{\mathrm{ds},i}$, thereby resulting in the effective gate voltage $V_{\mathrm{gs},i}$.

In the next step, for each slice we apply the model developed by Pregaldiny *et al.* [29, 30], which allows evaluation of the Si surface potential (ψ_s) and the carrier concentration with closed-form analytical expressions (note that these electrostatic quantities are needed to compute carrier DFs with formulas (1)-(9) as well as for the carrier mobility μ):

$$\begin{aligned} \psi_\mathrm{s} &= \phi + \frac{kT_\mathrm{B}}{q}\cdot\ln\left(\Theta - \frac{q\phi}{k_\mathrm{B}T}+1\right), \\ \Theta &= \left(V_{\mathrm{gs},i} - V_\mathrm{fb} - \phi - \frac{\psi_\mathrm{s,wi}-\phi}{\sqrt{1+\left(\dfrac{\psi_\mathrm{s,wi}-\phi}{4k_\mathrm{B}T/q}\right)^2}}\right)^2 \Bigg/ \\ &\Bigg/ \left(\gamma_\mathrm{body}\sqrt{\frac{k_\mathrm{B}T}{q}}\right)^2, \end{aligned} \tag{17}$$

where $\psi_\mathrm{s,wi}$ is the surface potential in the weak inversion mode:

$$\psi_\mathrm{s,wi} = \left(\sqrt{V_\mathrm{gs,i} - V_\mathrm{fb} + \gamma_\mathrm{body}^2/4} - \gamma_\mathrm{body}/2\right)^2 \tag{18}$$

and

$$\phi = \frac{\phi_\mathrm{B} + V_\mathrm{ch} + \psi_\mathrm{s,wi}}{2} - \frac{\sqrt{\psi_\mathrm{s,wi} - \phi_\mathrm{B} + 4\delta^2}}{2}, \tag{19}$$

where V_fb is the flatband voltage of the capacitor corresponding to the slice i; $\gamma_\mathrm{body} = \sqrt{2q\epsilon_\mathrm{Si}N_\mathrm{A/D}}/C_\mathrm{ox}$ is the body factor with $N_\mathrm{A/D}$ being the acceptor/donor concentration and C_ox the oxide capacitance; $\phi_\mathrm{B} = 2k_\mathrm{B}/q\cdot\ln\left(N_\mathrm{A/D}/n_\mathrm{int}\right)$ with the intrinsic carrier concentration n_int; V_ch is the quasi-Fermi level potential.

To evaluate the mobility we use a combination of low- and high-field mobility models [31, 32]. Note that these models are

implemented in the device simulator MINIMOS-NT [18] and results obtained with MINIMOS-NT were used as a reference.

The low-field electron mobility μ^{LIS} is modeled as:

$$\mu^{\mathrm{LIS}}(N_{\mathrm{D}}, N_{\mathrm{A}}) = \left(\frac{1}{\mu_{\mathrm{D}}(N_{\mathrm{D}})} + \frac{1}{\mu_{\mathrm{A}}(N_{\mathrm{A}})} - \frac{1}{\mu_0}\right)^{-1}, \quad (20)$$

where μ_{D} is the majority electron mobility, μ_{A} is the minority electron mobility, and μ_0 is the low-field mobility of electrons in the absence of dopants at room temperature.

The major mobility μ_{D} is evaluated as

$$\mu_{\mathrm{D}}(N_{\mathrm{D}}, T, Z_D) = \frac{\mu_0 - g - h}{1 + \left(\frac{N_{\mathrm{D}}}{C_1}\right)^{\alpha_1}} + \frac{g}{1 + \left(\frac{N_{\mathrm{D}}}{C_2}\right)^{\alpha_2}} + h \quad (21)$$

with

$$\mu_0(T) = 380 + 20700 \exp\left(-\frac{T}{100\mathrm{K}}\right), \quad (22)$$

$$g(T, Z) = 2\left(9 - 4\frac{Z}{Z_{\mathrm{P}}}\right) + \left(7\frac{Z}{Z_{\mathrm{P}}} + 208\right)\exp\left(-\frac{T}{200\mathrm{K}}\right), \quad (23)$$

$$h(T, Z) = \frac{9 - \frac{Z}{Z_{\mathrm{P}}}}{\frac{T}{300\mathrm{K}}}, \quad (24)$$

where μ_0 has dimensionality of $\mathrm{cm^2V^{-1}s^{-1}}$, temperature T is in K, N_{D} is the donor concentration, Z denotes the impurity atomic number, and Z_{P} = 15 is the atomic number for Phosphorous. As for the exponents α_1 and α_2, they are also given by empirical expressions:

$$\alpha_1(T) = 0.9 - 0.18\left(\frac{T}{300\mathrm{K}}\right), \quad (25)$$

$$\alpha_2(T) = 0.46 + 1.05\left(\frac{T}{300\mathrm{K}}\right). \quad (26)$$

Finally, the factors C_1 and C_2 with the dimensionality of $\mathrm{cm^{-3}}$ are evaluated as:

$$\frac{C_1}{10^{16}} = 11.85\left(\frac{T}{300\mathrm{K}}\right)^3 + 0.45 \quad (27)$$

$$\frac{C_2}{10^{20}} = \left[3 + \left(\frac{Z}{Z_{\mathrm{P}}}\right)^{-2}\right] \cdot \left[1.2 - \left(\frac{T}{300\mathrm{K}}\right)\exp\left(\frac{3 - 7\mathrm{T}}{300\mathrm{K}}\right)\right]. \quad (28)$$

The minority electron mobility is described in a similar manner:

$$\mu_{\mathrm{A}}(N_{\mathrm{A}}, T, Z_A) = \frac{\mu_0 + m - k - h}{1 + \left(\frac{N_{\mathrm{A}}}{C_1}\right)^{\alpha_1}} + \frac{k}{1 + \left(\frac{|N_{\mathrm{A}} - C_{\mathrm{a}}|}{C_2}\right)^{\alpha_2}} - \frac{m}{1 + \left(\frac{|N_{\mathrm{B}} - C_{\mathrm{b}}|}{C_3}\right)^{\alpha_3}}, \quad (29)$$

where N_{A} denotes the acceptor concentration and the other quantities are evaluated as

$$\alpha_3 = \frac{0.6}{\left(\frac{T}{300\mathrm{K}}\right)} + 1.4, \quad (30)$$

$$k(T) = \frac{134}{\left(\frac{T}{300\mathrm{K}}\right)} + 70, \quad (31)$$

$$m(T) = \frac{65}{\left(\frac{T}{300\mathrm{K}}\right)} + 73, \quad (32)$$

$$\frac{C_{\mathrm{a}}}{10^{19}} = 6\left[2 - 3\mathrm{exp}\left(-\frac{2.1T}{300\mathrm{K}}\right)\right], \quad (33)$$

$$\frac{C_{\mathrm{b}}}{10^{18}} = 6.7 - 12.9\left(\frac{T}{300\mathrm{K}}\right)^{0.25}\exp\left(-\frac{1.26T}{300\mathrm{K}}\right), \quad (34)$$

$$\frac{C_3}{10^{18}} = 2\left[300 + \exp\left(\frac{5.5T}{300\mathrm{K}}\right)\right]. \quad (35)$$

The values of $k(T)$ and $m(T)$ are in $\mathrm{cm^2V^{-1}s^{-1}}$, while the coefficients C_{a}, C_{b} and C_3 have the dimensionality of $\mathrm{cm^{-3}}$.

Then the impact of the electric field on the mobility is evaluated using the high-field mobility model [32]:

$$\mu^{\mathrm{LISF}} = \frac{2\mu^{\mathrm{LIS}}}{1 + \left[1 + \left(\frac{2\mu^{\mathrm{LIS}}F}{v_{\mathrm{sat}}}\right)^{\beta}\right]^{1/\beta}}, \quad (36)$$

where a dimensionless exponent β is assigned to be 2.217 as suggested by Grasser *et al.* [32] and F represents the driving force for electrons:

$$F = \left|\nabla\psi - \frac{1}{n}\nabla(k_{\mathrm{B}}T_{\mathrm{L}}n)\right|. \quad (37)$$

The first term is evaluated based on the gradient of the electrostatic potential ψ, i.e. it represents the drift component of the driving force, while the second term takes into account

non-uniformities in the carrier concentration and lattice temperature and therefore represents the diffusion component. If non-uniformities in lattice temperature (which can be related to self-heating) are neglected we can simplify the expression for the driving force:

$$F \approx \left| \nabla\psi - k_\mathrm{B} T_\mathrm{L} \frac{\nabla(n)}{n} \right|. \tag{38}$$

The gradients of the electrostatic potential and the carrier concentrations are evaluated using the slicing of the device depicted in Fig. 2.

VII. Modeling of Degraded Devices

The effect of generated interface traps is twofold: they perturb the device electrostatics and degrade the carrier mobility. The drain current and its change are expressed as

$$\begin{aligned} I &= \sigma V_\mathrm{ds} \\ \Delta I &= \Delta(\sigma) V_\mathrm{ds}, \end{aligned} \tag{39}$$

where σ is the overall conductivity of the transistor which is divided into slices (see Fig. 2) and each slice with an index i is characterized by a mobility σ_i; then the overall conductivity reads as

$$\sigma = \left[\sum_i 1/\sigma_i \right]^{-1} = \left[\sum_i \frac{1}{q n_i \mu_i} \right]^{-1}, \tag{40}$$

where n_i denotes the electron concentration in the segment i and μ_i is the carrier mobility in this segment; q is the elementary charge. Therefore, the change in the drain current due to generated interface traps is:

$$\Delta I \sim \Delta \left(\left[\sum_i \frac{1}{q n_i \mu_i} \right]^{-1} \right) V_\mathrm{ds} \tag{41}$$

Here, the distortion in the carrier concentration is evaluated within the model developed by Pregaldiny *et al.* [29, 30] by introducing a gate voltage perturbation $\delta V_{\mathrm{gs},i} \sim N_\mathrm{it}/C_\mathrm{ox}$ (where C_ox is the sheet capacitance) and then calculating electrostatic quantities using formulas summarized in the Section VI.

As for mobility degradation, we model the degraded mobility as [12]:

$$\mu_\mathrm{degr} = \frac{\mu_\mathrm{fresh}}{(1 + \alpha N_\mathrm{it})} \tag{42}$$

with $\alpha = 10^{-13}\mathrm{cm}^{-2}$ and μ_fresh being the mobility in the fresh FET.

Using this analytical model we were able to accurately reproduce measured $\Delta I_\mathrm{d,lin}(t)$ traces, see Fig. 6. As a reference, we also show $\Delta I_\mathrm{d,lin}(t)$ dependencies obtained with the TCAD version of the HCD model; one can see that both models result in very similar degradation characteristics. Although in TCAD and Comphy implementations values of the parameters of the Si-H bond rupture process are slightly different they are still in good agreement (see Fig. 5). It is important to emphasize that *all expressions of all modules of the compact physics model are analytic* and no additional TCAD simulations are required.

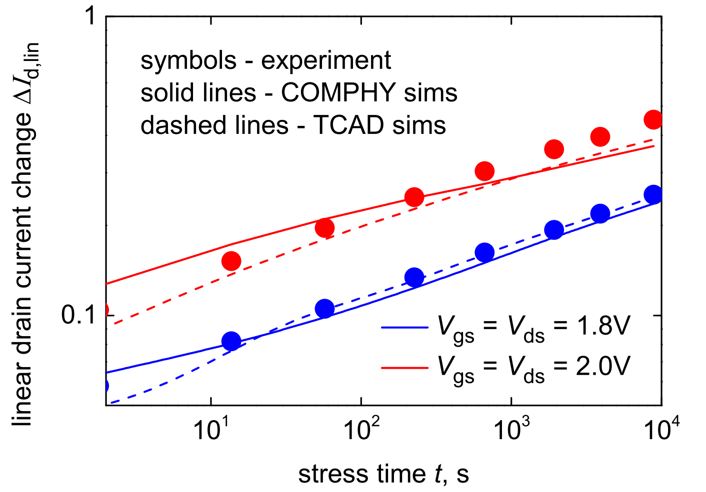

Fig. 6. Normalized $\Delta I_\mathrm{d,lin}$ changes as functions of stress time t: experiment vs. modeling. Note that two versions of the model are used, i.e. the compact physics model (Comphy) and the full TCAD version.

VIII. Conclusions

We developed a compact physics model for hot-carrier degradation. The model incorporates three main modules: carrier transport description, calculations of defect generation rates, and modeling of the degraded devices. All the aspects of the HCD problem are modeled using *only analytical expressions*. The model was validated against experimental data acquired from n-channel MOSFETs with a gate length of 65 nm stressed at the worst-case conditions and was shown to represent experimental changes in the linear drain current with good accuracy.

IX. Acknowledgements

This work was supported in part by the European Union's Horizon 2020 research and innovation programme under the Marie Sklodowska-Curie grant agreement No. 794950 and by the Austrian Science Fund (FWF), grant No. P31204-N30.

The authors are thankful to Jacopo Franco, Erik Bury, and Zhicheng Wu for stimulating discussions.

References

[1] S. Novak, C. Parker, D. Becher, M. Liu, M. Agostinelli, M. Chahal, P. Packan, P. Nayak, S. Ramey, and S. Natarajan, "Transistor Aging and Reliability in 14nm Tri-gate Technology," in *2015 IEEE International Reliability Physics Symposium*, April 2015, pp. 2F.2.1–2F.2.5.

[2] A. Rahman, J. Dacuna, P. Nayak, G. Leatherman, and S. Ramey, "Reliability Studies of a 10nm High-performance and Low-power CMOS Technology Featuring 3rd Generation FinFET and 5th Generation HK/MG," in *2018 IEEE International Reliability Physics Symposium (IRPS)*, March 2018, pp. 6F.4–1–6F.4–6.

[3] S. Tyaginov, I. Starkov, H. Enichlmair, J. Park, C. Jungemann, and T. Grasser, "Physics-Based Hot-Carrier Degradation Models (invited)," *ECS Transactions*, vol. 35, no. 4, pp. 321–352, 2011.

[4] A. Bravaix, C. Guerin, V. Huard, D. Roy, J. Roux, and E. Vincent, "Hot-carrier Acceleration Factors for Low Power Management in DC-AC Stressed 40nm NMOS Node at High Temperature," in *Proc. International Reliability Physics Symposium (IRPS)*, 2009, pp. 531–546.

[5] C. Guerin, V. Huard, and A. Bravaix, "General Framework about Defect Creation at the Si/SiO_2 Interface," *Journal of Applied Physics*, vol. 105, pp. 114 513–1–114 513–12, 2009.

[6] Y. Randriamihaja, X. Federspiel, V. Huard, A. Bravaix, and P. Palestri, "New Hot Carrier Degradation Modeling Reconsidering the Role of EES in Ultra Short n-channel MOSFETs," in *Proc. International Reliability Physics Symposium (IRPS)*, 2013, pp. 1–5.

[7] S. Reggiani, G. Barone, E. Gnani, A. Gnudi, G. Baccarani, S. Poli, R. Wise, M.-Y. Chuang, W. Tian, S. Pendharkar, and M. Denison, "Characterization and Modeling of Electrical Stress Degradation in STI-based Integrated Power Devices," *Solid-State Electronics*, vol. 102, no. 12, pp. 25–41, 2014.

[8] A. N. Tallarico, S. Reggiani, R. Depetro, A. M. Torti, G. Croce, E. Sangiorgi, and C. Fiegna, "Hot-Carrier Degradation in Power LDMOS: Selective LOCOS- Versus STI-Based Architecture," *IEEE Journal of the Electron Devices Society*, vol. 6, no. 1, pp. 219–226, 2018.

[9] S. Tyaginov, M. Bina, J. Franco, Y. Wimmer, D. Osintsev, B. Kaczer, and T. Grasser, "A Predictive Physical Model for Hot-Carrier Degradation in Ultra-Scaled MOSFETs," in *Proc. Simulation of Semiconductor Processes and Devices (SISPAD)*, 2014, pp. 89–92.

[10] S. Tyaginov, M. Jech, J. Franco, P. Sharma, B. Kaczer, and T. Grasser, "Understanding and Modeling the Temperature Behavior of Hot-Carrier Degradation in SiON nMOSFETs," *IEEE Electron Device Letters*, vol. 37, no. 1, pp. 84–87, Jan 2016.

[11] A. Makarov, S. E. Tyaginov, B. Kaczer, M. Jech, A. Chasin, A. Grill, G. Hellings, M. I. Vexler, D. Linten, and T. Grasser, "Hot-Carrier Degradation in FinFETs: Modeling, Peculiarities, and Impact of Device Topology," in *2017 IEEE International Electron Devices Meeting (IEDM)*, Dec 2017, pp. 13.1.1–13.1.4.

[12] P. Sharma, S. Tyaginov, Y. Wimmer, F. Rudolf, K. Rupp, M. Bina, H. Enichlmair, J.-M. Park, R. Minixhofer, H. Ceric, and T. Grasser, "Modeling of Hot-Carrier Degradation in nLDMOS Devices: Different Approaches to the Solution of the Boltzmann Transport Equation," *IEEE Transactions on Electron Devices*, vol. 62, no. 6, pp. 1811–1818, 2015.

[13] P. Sharma, M. Jech, S. Tyaginov, F. Rudolf, K. Rupp, H. Enichlmair, J. M. Park, and T. Grasser, "Modeling of hot-carrier degradation in LDMOS devices using a drift-diffusion based approach," in *2015 International Conference on Simulation of Semiconductor Processes and Devices (SISPAD)*, Sept 2015, pp. 60–63.

[14] P. Sharma, S. Tyaginov, S. E. Rauch, J. Franco, A. Makarov, M. I. Vexler, B. Kaczer, and T. Grasser, "Hot-Carrier Degradation Modeling of Decananometer nMOSFETs Using the Drift-Diffusion Approach," *IEEE Electron Device Letters*, vol. 38, no. 2, pp. 160–163, Feb 2017.

[15] Z. Wu, J. Franco, P. Roussel, S. Tyaginov, B. Truijen, M. Vandemaele, G. Hellings, N. Collaert, G. Groeseneken, D. Linten, and B. Kaczer, "A Physics-Aware Compact Modeling Framework of Transistor Aging Across the Entire Bias Space," in *Proc. International Electron Devices Meeting (IEDM), in press*.

[16] G. Rzepa, J. Franco, B. O'Sullivan, A. Subirats, M. Simicic, G. Hellings, P. Weckx, M. Jech, T. Knobloch, M. Waltl, P. Roussel, D. Linten, B. Kaczer, and T. Grasser, "Comphy — A compact-physics framework for unified modeling of BTI," *Microelectronics Reliability*, vol. 85, pp. 49–65, 2018. [Online]. Available: http://www.sciencedirect.com/science/article/pii/S0026271418301641

[17] M. Bina, K. Rupp, S. Tyaginov, O. Triebl, and T. Grasser, "Modeling of Hot Carrier Degradation Using a Spherical Harmonics Expansion of the Bipolar Boltzmann Transport Equation," in *Proc. International Electron Devices Meeting (IEDM)*, 2012, pp. 713–716.

[18] T. B. Stockinger, K. Dragosits, T. Grasser, R. Klima, M. Knaipp, H. Kosina, R. Mlekus, V. Palankovski, M. Rottinger, G. Schrom, S. Selberherr, and M., *MINIMOS-NT User's Guide*, Institut für Mikroelektronik, 1998.

[19] *http://www.globaltcad.com/en/products/minimos-nt.html*.

[20] T. Grasser, H. Kosina, C. Heitzinger, and S. Selberherr, "Accurate Impact Ionization Model which Accounts for Hot and Cold Carrier Populations," *Applied Physics Letters*, vol. 80, no. 4, pp. 613–615, 2002.

[21] M. Jech, B. Ullmann, G. Rzepa, S. Tyaginov, A. Grill, M. Waltl, D. Jabs, C. Jungemann, and T. Grasser, "Impact of Mixed Negative Bias Temperature Instability and Hot Carrier Stress on MOSFET Characteristics—Part II: Theory," *IEEE Transactions on Electron Devices*, vol. 66, no. 1, pp. 241–248, Jan 2019.

[22] S. Tyaginov, I. Starkov, O. Triebl, J. Cervenka, C. Jungemann, S. Carniello, J. Park, H. Enichlmail, C. Kernstock, E. Seebacher, R. Minixhofer, H. Ceric, and T. Grasser, "Interface Traps Density-of-states as a Vital Component for Hot-carrier Degradation Modeling," *Microelectronics Reliability*, vol. 50, pp. 1267–1272, 2010.

[23] S. Tyaginov, M. Bina, J. Franco, D. Osintsev, O. Triebl, B. Kaczer, and T. Grasser, "Physical Modeling of Hot-Carrier Degradation for Short- and Long-Channel MOSFETs," in *Proc. International Reliability Physics Symposium (IRPS)*, 2014, pp. XT.16–1–16–8.

[24] K. Brower, "Dissociation Kinetics of Hydrogen-Passivated (111)Si-$Si0_2$ Interface Defects," *Physical Review B*, vol. 42, no. 6, pp. 3444–3454, 1990.

[25] A. Stesmans, "Revision of H_2 Passivation of P_2 Interface Defects in Standard (111)Si/SiO_2," *Applied Physics Letters*, vol. 68, no. 19, pp. 2723–2725, 1996.

[26] ——, "Passivation of P_{b0} and P_{b1} Interface Defects in Thermal (100) Si/SiO_2 with Molecular Hydrogen," *Appl. Phys. Lett.*, vol. 68, no. 15, pp. 2076–2078, 1996.

[27] G. Pobegen, S. Tyaginov, M. Nelhiebel, and T. Grasser, "Observation of Normally Distributed Activation Energies for the Recovery from Hot Carrier Damage," *IEEE Electron Dev. Lett.*, vol. 34, no. 8, pp. 939–941, 2013.

[28] M. Bina, S. Tyaginov, J. Franco, Y. Wimmer, D. Osinstev, B. Kaczer, T. Grasser, *et al.*, "Predictive Hot-Carrier Modeling of n-channel MOSFETs," *IEEE Transactions on Electron Devices*, vol. 61, no. 9, pp. 3103–3110, 2014.

[29] F. Prégaldiny, C. Lallement, and D. Mathiot, "Accounting for quantum mechanical effects from accumulation to inversion, in a fully analytical surface-potential-based MOSFET model," *Solid-State Electronics*, vol. 48, no. 5, pp. 781–787, 2004. [Online]. Available: http://www.sciencedirect.com/science/article/pii/S0038110103004313

[30] F. Prégaldiny, C. Lallement, R. van Langevelde, and D. Mathiot, "An advanced explicit surface potential model physically accounting for the quantization effects in deep-submicron MOSFETs," *Solid-State Electronics*, vol. 48, no. 3, pp. 427–435, 2004. [Online]. Available: http://www.sciencedirect.com/science/article/pii/S0038110103003575

[31] G. Kaiblinger-Grujin, T. Grasser, and S. Selberherr, "A Physically-Based Electron Mobility Model for Silicon Device Simulation," in *Proc. International Conference on Simulation of Semiconductor Processes and Devices (SISPAD)*, 1998, pp. 312–315.

[32] T. Grasser, K. Tsuneno, S. Selberherr, and H. Masuda, "Mobility Parameter Tuning for Device Simulation," in *28th European Solid-State Device Research Conference*, Sep. 1998, pp. 336–339.